Substituent and Solvent Effects on the Hyperporphyrin Spectra of Diprotonated Tetraphenylporphyrins†

James R. Weinkauf, Sharon W. Cooper, Aaron Schweiger, and Carl C. Wamser*

Department of Chemistry, Portland State University, Portland, Oregon 97207-0751

Received: September 11, 2002; In Final Form: November 13, 2002

UV−visible spectra have been studied for a series of p-substituted tetraphenylporphyrins (TPPs) titrated with strong acid in various solvents. Substituent effects on the Soret and *Q*(*I*) absorption peaks and the fluorescence emission peaks have been treated by Hammett correlations. In general, there are only small effects with electron-withdrawing substituents, but electron-donating substituents lead to lower energy transitions, with especially strong effects observed in the case of the diprotonated porphyrins with good electron-donating substituents (hyperporphyrin effects). The hyperporphyrin effects are attributed to the crossing of a π molecular orbital on the substituted phenyl group above the usual porphyrin π highest occupied molecular orbital. For the neutral TPPs, this crossing is estimated to occur with a substituent as electron-donating as *p*-methoxy, and for the diprotonated TPPs, the crossing occurs at approximately unsubstituted TPP. Distinctive solvent effects on the spectra and the Hammett correlations are observed.

Introduction

Porphyrins have a wonderful repertoire of optical and electronic properties that allow them to play a variety of roles, in nature and in technical applications.[1] The spectroscopy of porphyrins has received detailed treatment because of its relevance to functionality as well as its fascinating variety.[2] In the ultraviolet−visible region, the characteristic spectrum includes the intense Soret band around 400 nm and a series of bands (Q bands) through the visible range. Different patterns of peripheral substitutions, π conjugations, or central metal incorporations lead to well-characterized spectral patterns.[2] Specialized spectral features also appear based on interactions between porphyrin units, such as H and J aggregates[3] or interactions with other molecules based on charge, π stacking, H-bonding, or hydrophobic effects.[4,5] The Gouterman four orbital model suffices to explain most of the fundamental features of porphyrin and metalloporphyrin electronic spectra,[2] but there are increasingly common examples of unusual spectral features that require additional interpretation.

Acid−base behavior of porphyrins has also been well-studied. The tetrapyrrole skeleton allows for loss of two N−H protons to form a dianion in strong base or gain of two protons to form a dication in acid. Each case leads to an increase in symmetry and corresponding changes in the spectra, which are often distinctive in their colors (e.g., purple tetraphenylporphyrins (TPPs) change to green in acid). Moreover, peripheral substituents may confer additional acidic or basic properties, a tactic often used to control water solubility.[4]

The basic structure of the porphyrin framework can be described as a planar aromatic system, but steric effects around the periphery, in particular meso substituents that interact with β pyrrole positions, often lead to nonplanar forms of porphyrins.[6] TPP has been observed in three different crystal forms, but in each case, the meso phenyl groups are significantly twisted from the plane of the porphyrin.[7] The X-ray structure of doubly protonated TPP[8] shows a nonplanar (saddle) form, in which the four N−H bonds adopt positions alternately above and below the mean porphyrin plane; this twisting allows the phenyl rings to become more coplanar with the mean molecular plane. Thus, it has been of some interest to determine the extent to which peripheral substituents can interact with the central porphyrin positions, where the charges are nominally located.

Systematic effects of para substituents on the properties of TPPs have been studied electrochemically[9,10] and spectroscopically.[11−13] In general, electron-donating substituents lead to red shifts for both the Soret (B) and Q bands, maintaining approximately a constant B−Q splitting.[13] The magnitude of the energy shifts can be correlated with Hammett substituent constants, either a mix of resonance and inductive components[12] or σ^+ values.[13] Substituent effects on the redox potentials[9,10] and pK_a values[12] also correlate with Hammett substituent constants.

Nevertheless, several studies of TPPs substituted with highly electron-donating groups have shown unusual spectroscopic effects. Studies with para-hydroxy TPP derivatives have illustrated numerous spectral and structural features, complicated by accompanying redox processes leading to paramagnetic species and quinonelike structures.[14−16] Para-amino TPP derivatives have long been known to have unusual spectral properties, in particular broader, lower energy bands for both the Soret and the visible regions.[17,18] Protonation of these amino-substituted derivatives leads to further red shifts and unusual red bands. For example, tetrakis(*p*-dimethylaminophenyl)porphyrin (TDMAPP) can be titrated with acid to show protonated derivatives from +2 to +6.[19] The diprotonated form shows an unusually intense red band, described as a hyperporphyrin. A similar band has been observed in long chain dialkylamino-substituted porphyrins in thin films.[20]

Hyperporphyrins have been defined as porphyrins that exhibit extra bands in the UV−visible, either due to specific interactions with metal orbitals or due to charge transfer interactions with substituents.[2] Molecular orbital calculations supporting the charge transfer nature of hyperporphyrin bands in diprotonated

† Part of the special issue "George S. Hammond & Michael Kasha Festschrift".

10.1021/jp022046f CCC: $25.00 © 2003 American Chemical Society
Published on Web 12/20/2002

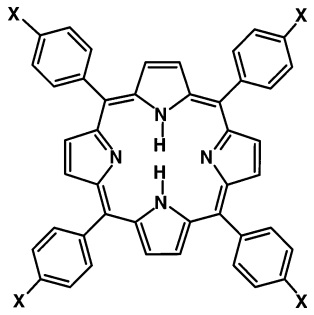

Figure 1. Tetrasubstituted porphyrins and abbreviations. TPP, X = H; TTP, X = CH_3; THPP, X = OH; TMPP, X = OCH_3; TAPP, X = NH_2; TDMAPP, X = $N(CH_3)_2$; TNPP, X = NO_2; TCPP, X = COOH; TCMPP, X = CO_2CH_3. Mixed substituent porphyrins: H_nM_mPP, X = OH or OCH_3; H_1M_3PP, H_2M_2PP, H_3M_1PP. DMA_nPP, X = H or $N(CH_3)_2$; DMA_1PP, DMA_2PP, DMA_3PP.

TAPP have recently been presented.[21] We have collected UV−visible absorption and fluorescence spectroscopy data on a series of substituted TPPs (Figure 1) to categorize the effects of substituents on the spectra. We have also investigated the role of solvent effects on the spectra.

Experimental Section

Materials. Solvents and reagents were typically the highest grade commercially available and were stored under nitrogen with molecular sieves. Methanol (MeOH), acetonitrile (ACN), and tetrahydrofuran (THF) were Sigma-Aldrich high-performance liquid chromatography (HPLC) grade, 99.9% with no inhibitors. Dimethyl sulfoxide (DMSO) and dimethylformamide (DMF) were Aldrich spectrometric grade, 99.9 and 99.8%, respectively. Dichloromethane (DCM) was from Mallinckrodt, indicating 0.0007 mequiv/g titratable acid; however, this source of DCM did not detectably protonate the porphyrins, a common problem with most chlorinated solvents from most other sources. Acids used for titrations were either trifluoroacetic acid (TFA) or methanesulfonic acid (MSA). TFA was from Aldrich, 99+% spectrometric grade, and MSA was from J. T. Baker, 98%. Water was distilled water available in the lab, boiled before use.

All of the porphyrins used were tetrasubstituted in their meso positions with para-substituted phenyl groups. The various symmetrically substituted porphyrins used in this study are shown in Figure 1. The porphyrins were either purchased commercially or synthesized by standard techniques. TPP was purchased from Strem Chemicals (Newburyport, MA), TCPP and TCMPP were purchased from Porphyrin Products (now Frontier Scientific, Logan, UT), and TAPP was purchased from TCI America (Portland, OR). THPP was prepared by demethylating TMPP using pyridinium hydrochloride.[22] TTP, TMPP, and TNPP were prepared from pyrrole and the corresponding para-substituted benzaldehyde by the standard Adler−Longo procedure,[23] and TDMAPP was prepared by a slightly modified procedure.[19]

Porphyrins containing different substituents were prepared in the cases of H_nM_mPP (hydroxy or methoxy substituents) and DMA_nPP (dimethylamino substituents or unsubstituted positions). Syntheses of the DMA_nPP series have been reported.[19] The H_nM_mPP series was prepared by the Adler−Longo procedure with a mix of benzaldehydes and chromatographic separation of the various derivatives as follows.

Preparation of Hydroxy/Methoxy-Substituted TPPs. *HM_3PP*. *para*-Hydroxybenzaldehyde (2.0 g, 16 mmol), previously recrystallized from 3:1 acetone:toluene, was added to 250 mL of propionic acid and brought to reflux. Pyrrole (6.2 mL, 89 mmol) was added, followed by *para*-methoxybenzaldehyde (8.9 mL, 73 mmol), and the solution was stirred at reflux for 45 min. The reaction mixture was allowed to cool to room temperature and then placed in an ice bath, yielding purple crystals. Thin-layer chromatography (TLC) indicated two major components, identified as TMPP and HM_3PP. Several milligrams of pure HM_3PP were isolated by flash chromatography using toluene/chloroform solutions as eluting solvents. NMR ($CDCl_3$): −2.75 ppm (s, 2H, NH), 4.09 ppm (s, 9H, OCH_3), 7.20 ppm (d, 2H, *H*-ArOH), 7.28 ppm (d, 6H, *H*-$ArOCH_3$), 8.07 ppm (d, 2H, *H*-ArOH), 8.14 ppm (d, 6H, *H*-$ArOCH_3$), 8.86 ppm (broad singlet, 8H, pyrroles). ICR-MS: M + 1 = 721.25 (calcd 721.297).

H_2M_2PP and H_3MPP. Although the above preparation yielded traces of other porphyrins, improved yields of the other substituted derivatives were obtained by using a different ratio of the two benzaldehydes. The above procedure was modified by using *para*-hydroxybenzaldehyde (2.5 g, 20 mmol), *para*-methoxybenzaldehyde (4.5 mL, 37 mmol), and pyrrole (5.5 mL, 80 mmol). The reaction mixture did not yield crystals but a thick tar, which was treated with toluene and filtered. The toluene solution was evaporated, and the solid residue was chromatographed several times on silica gel using chloroform eluent and then 1−5% MeOH in chloroform. The cis and trans isomers of H_2M_2PP were not separated.

H_2M_2PP. NMR ($CDCl_3$): −2.75 ppm (s, 2H, NH), 4.12 ppm (s, 6H, OCH_3), 7.23 ppm (d, 4H, *H*-ArOH), 7.30 ppm (d, 4H, *H*-$ArOCH_3$), 8.09 ppm (d, 4H, *H*-ArOH), 8.14 ppm (d, 4H, *H*-$ArOCH_3$), 8.86 ppm (broad singlet, 8H, pyrroles). MALDI-MS: M + 1 = 707.27 (calcd 707.266).

H_3MPP. NMR ($CDCl_3$): −2.76 ppm (s, 2H, NH), 4.12 ppm (s, 3H, OCH_3), 7.23 ppm (d, 6H, *H*-ArOH), 7.31 ppm (d, 2H, *H*-$ArOCH_3$), 8.09 ppm (d, 6H, *H*-ArOH), 8.14 ppm (d, 2H, *H*-$ArOCH_3$), 8.88 ppm (broad singlet, 8H, pyrroles). MALDI-MS: M + 1 = 693.27 (calcd 693.250).

Spectroscopy. UV−visible absorption spectra were taken on a Shimadzu model 260 using a 2 mm slit width. Data acquisition was via a GPIB card and a PC using Shimadzu UV-265 software (version 3.1). Fluorescence spectra were taken on a Spex Fluorolog model 112 spectrofluorimeter using a 150 W xenon light source and right angle detection with optically dilute samples (<1 μM). For emission spectra, the excitation slit width was 5 mm and the emission slit width was 0.5 mm. The reverse was set for excitation spectra. For determination of relative emission intensities, excitation was at the isosbestic point of the neutral and diprotonated porphyrins to allow for equivalent absorbance. All spectra were plotted and analyzed with Igor Pro (version 3.01). Fluorescence lifetimes were measured for a few selected samples at Jobin Yvon-Spex, using a Spex Fluorolog τ fluorimeter. Ion cyclotron resonance mass spectrometry (ICR-MS) was performed at the Pacific Northwest National Laboratories using electrospray ionization. Matrix-assisted laser desorption−ionization mass spectrometry (MALDI-MS) was performed at Washington State University.

Titrations. Porphyrins were protonated by strong acid (either MSA or TFA) by titrations in a UV cuvette while monitoring the spectra between 300 and 900 nm. Neat or concentrated solutions of acid were added in 2 μL aliquots using a Gilson 20 μL Pipetman micropipet. The original porphyrin solution was 6 μM or less in a total volume of 3.0 mL; corrections were not made for change in total volume during the titration (typically less than 100 μL). After addition of each aliquot, the cell was capped and mixed by inversion, and the spectrum was

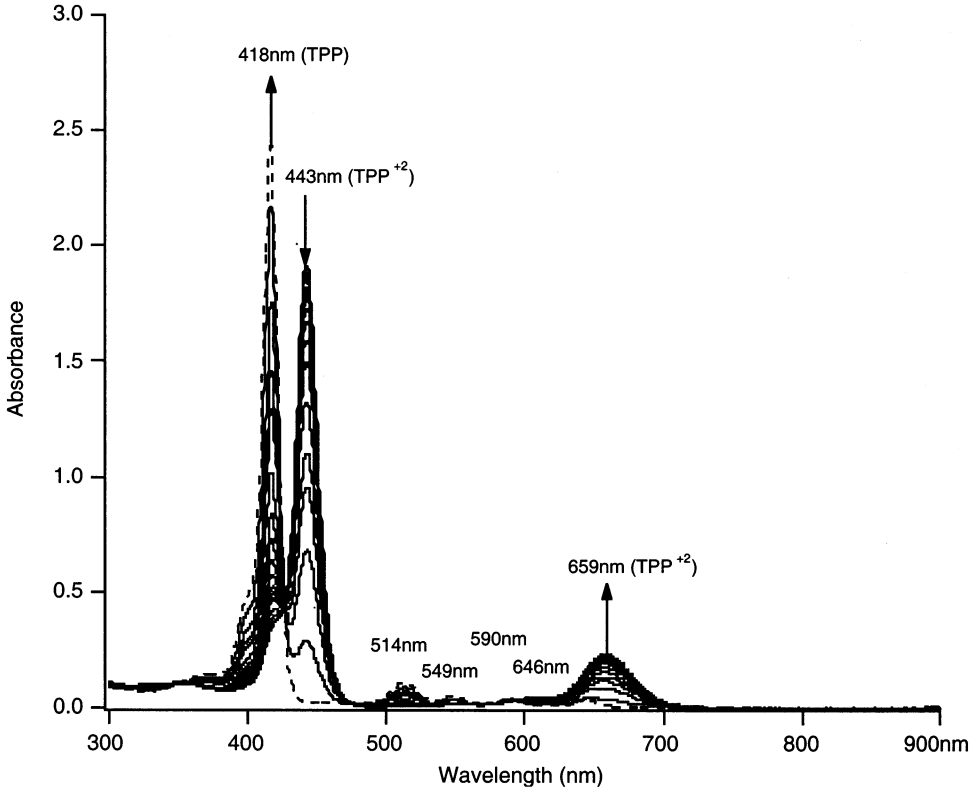

Figure 2. Titration of 5.23 μM TPP with MSA in DMSO.

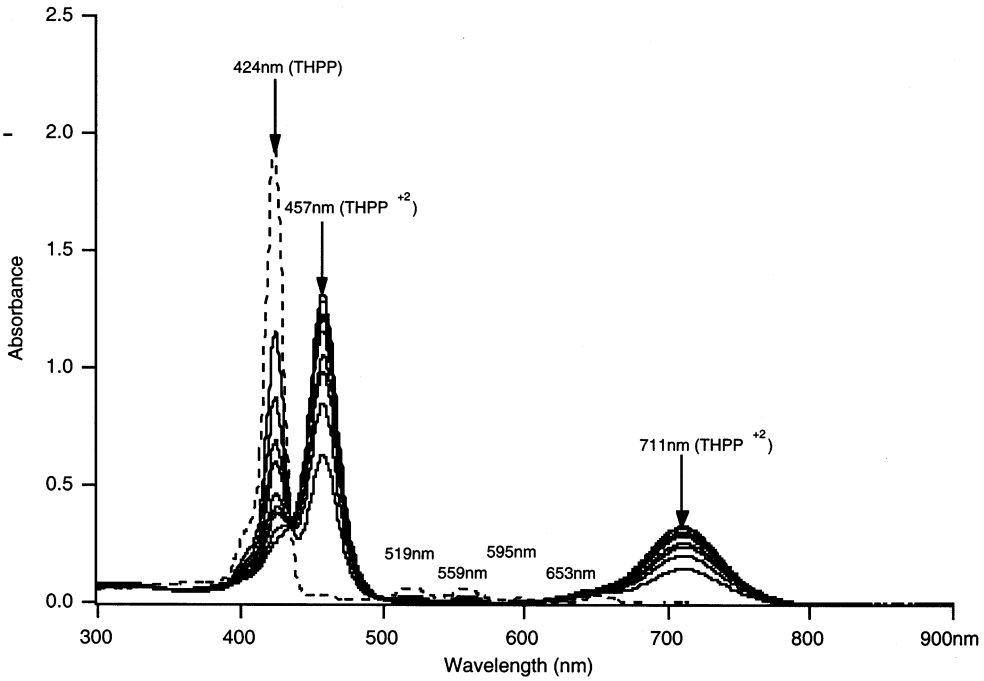

Figure 3. Titration of 5.84 μM THPP with TFA in DMSO.

retaken. In several cases, the reversibility of the protonation was demonstrated by addition of 1.0 M tetrabutylammonium hydroxide in MeOH.

Results

Porphyrin Absorption and Emission Spectra. For reference, the normal UV−visible spectroscopic characteristics of the *meso*-tetraarylporphyrins and their diprotonated forms are illustrated in Figure 2 for unsubstituted TPP. Protonation leads to a red shift and weakening of the Soret band, disappearance of most of the Q bands due to higher symmetry, and for the *Q*(*I*) band, a small red shift (646−659 nm) with a substantially increased intensity.

For tetraarylporphyrins with good electron-donating substituents, a modified pattern is observed upon protonation, as illustrated in Figure 3 for THPP. Effects on the Soret band and the Q bands are relatively similar to what is observed for TPP, except for the *Q*(*I*) band, which is more strongly red-shifted and more strongly increased in intensity. A similar red shift is

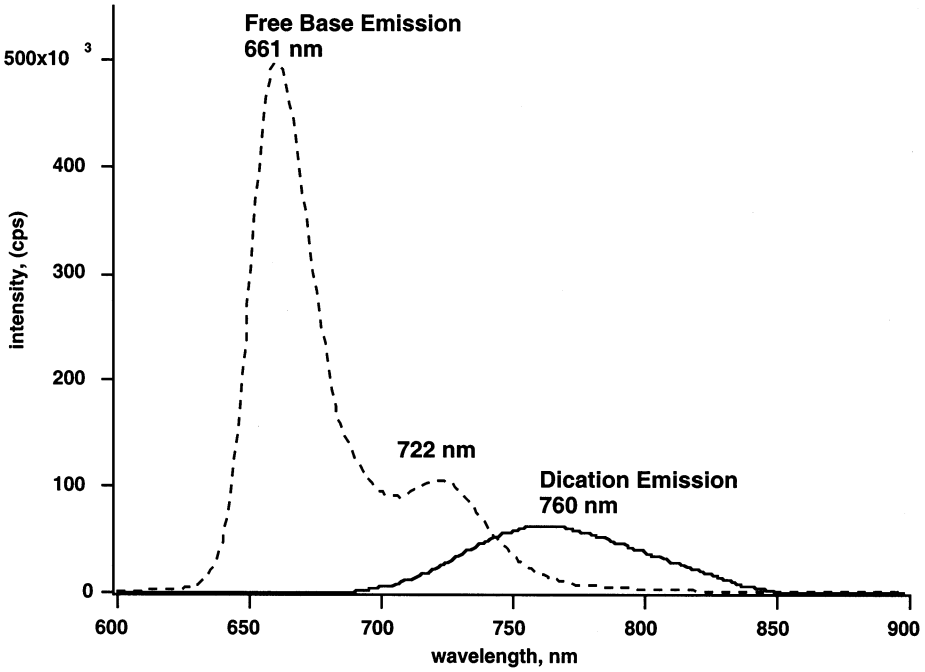

Figure 4. Fluorescence spectra of 0.78 μM THPP in DMSO.

observed in the fluorescence spectrum, but the emission intensity is substantially reduced, as illustrated in Figure 4 for neutral and diprotonated THPP.

For even more strongly electron-donating substituents, in particular amino substituents, the trends are even more striking. The complete titration of TAPP with MSA in DMSO is illustrated in Figure 5, revealing protonation states +2 through +6, completely analogous to what was observed by Ojadi et al. for TDMAPP.[19] The longest wavelength absorption at 811 nm, however, is the greatest shift we have found for any diprotonated substituted TPP. The magnitude of the shift is enhanced by a solvent effect, as discussed in the next section. Diprotonated TAPP can be observed to fluoresce weakly in DCM solvent but not in DMSO. Fluorescence from diprotonated TDMAPP has not been detected in any solvent.

Substituent Effects. In an effort to better understand the role of electron-donating substituents in the generation of hyperporphyrin spectra, a series of para-substituted porphyrins were prepared and titrated with acid. The observed effects on the peak positions of the Soret bands, the *Q*(*I*) bands, and the fluorescence emission are summarized in Table 1.

The data from Table 1 were plotted as a function of Hammett substituent constant (4σ, since there are four substituents), using either the standard σ values or σ^+ values (Figures 6−9). Summary results are collected in Table 2.

The Hammett correlations in Figures 6−9 include data for the Soret and *Q*(*I*) bands for both the neutral and the diprotonated forms, in both DCM and DMSO solvents. Slopes (ρ values) were obtained using energy as the *y*-axis, consistent with the typical expression of Hammett correlations as linear free energy relationships. Data in additional solvents are summarized in the following section, but these two solvents are both representative and distinctive, especially for the most extreme (amino-substituted) hyperporphyrin behavior. Peak fluorescence emission wavelengths for the diprotonated forms are also presented to get an alternative tracking of the lowest excited states.

Substituent effects on the neutral absorption bands correlate better with σ rather than σ^+ values. The Soret band shows a red shift, relative to unsubstituted TPP, for either electron-donating or electron-withdrawing solvents, i.e., there is a break in the Hammett plot at TPP. The electron-donating effect is much stronger ($\rho = +1.2/-0.4$ in DCM; $+1.5/-0.4$ in DMSO). For the *Q*(*I*) band, the substituent effects are smaller, with no significant shifts for electron-withdrawing substituents ($\rho =$ +0.4/0 in DCM; +0.7/0 in DMSO).

Substituent effects on the dication absorption and emission bands correlate better with σ^+ rather than σ values. If the data are plotted vs σ, dication Soret bands show a red shift for either electron-donating or electron-withdrawing solvents, extremely similar to what is observed for the neutral Soret data. Dication Soret data are plotted vs σ^+ using only the electron-donating substituents, since electron-withdrawing substituents have σ^+ values very similar to their σ values. As compared to the ρ values from plots vs σ, ρ^+ values are smaller, but this is an artifact of the larger values of σ^+ relative to σ ($\rho^+ = +0.65$ in DCM; +0.61 in DMSO). For the *Q*(*I*) band, the effects are larger ($\rho^+ = +0.9$ in both DCM and DMSO). However, the data for diprotonated TAPP *Q*(*I*) in DMSO fall distinctly off the linear correlation, with the red shift under those conditions much larger than expected.

Solvent Effects. To help clarify the role of solvent in the observed spectra, each of the substituted TPP derivatives was studied in a variety of solvents and Hammett correlations were plotted for each solvent. Table 3 indicates the different solvent parameters that were considered when attempting to correlate the effects on the spectra. None were very effective at revealing correlations with the observed spectral shifts, but the E_T (30) scale was considered the best as well as the most relevant, since it is derived from a solvent-induced shift in the position of a charge transfer absorption band.[24] E_T^N is a similar scale, normalized to the full range of polarity observed for E_T (30).

Figures 10 and 11 show the data for Soret and *Q*(*I*) band positions for both neutral and diprotonated forms of TPP and four derivatives with electron-donating substituents, in six different solvents. The Soret bands show a slight trend toward increasing energy in more polar solvents, although the scatter is substantial. The *Q*(*I*) band correlations are remarkably flat, with similarly large scatter. Noteworthy, however, are the data for diprotonated TAPP, which scatter widely over a large energy

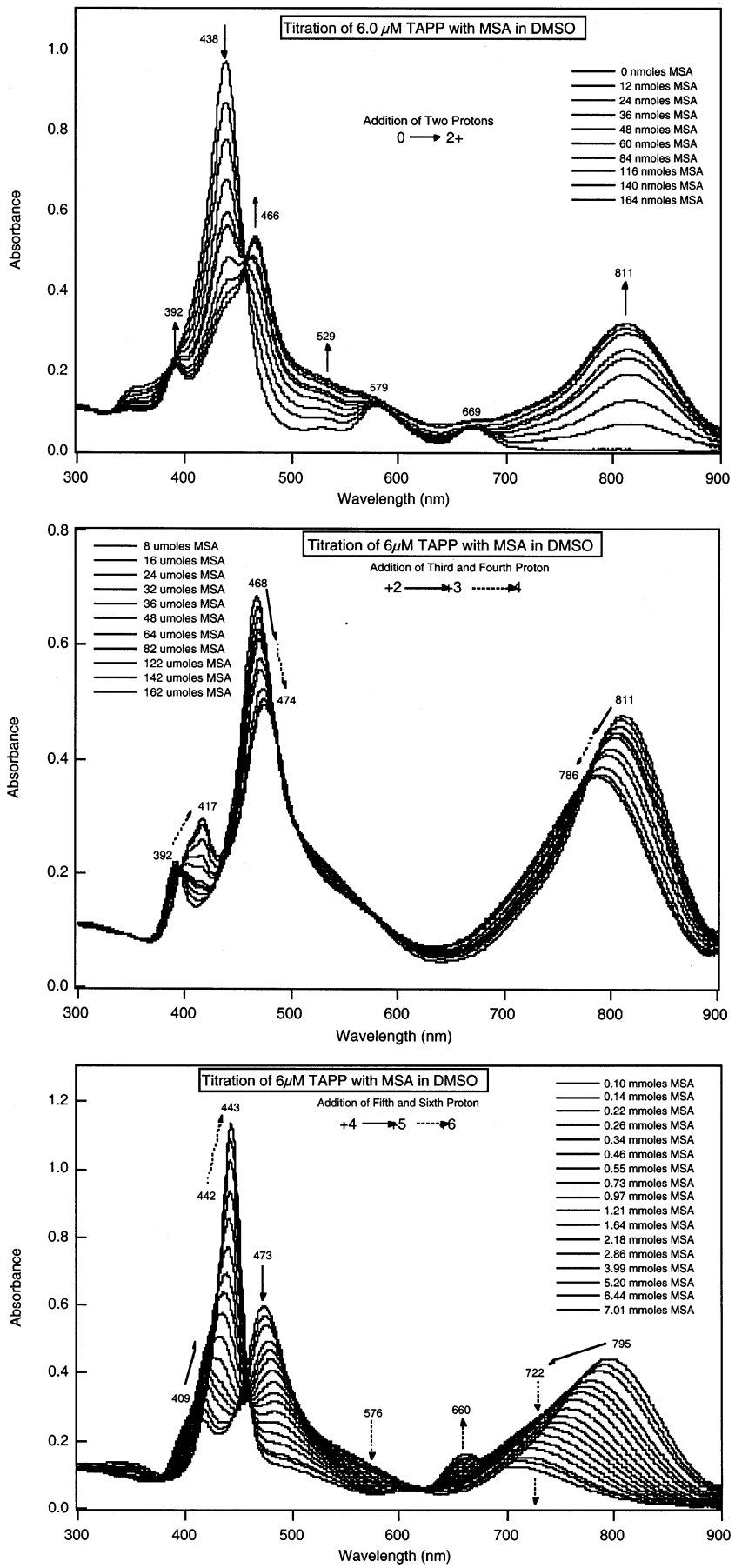

Figure 5. Titration of 6.0 μM TAPP with MSA in DMSO, revealing various stages of protonation.

TABLE 1: Absorption and Fluorescence Data for Substituted TPPs (First Entry in DCM Solvent/Second Entry in DMSO Solvent, NA = Data Not Available)

Absorption Data

		Hammett		Soret (nm)			*Q*(*I*) (nm)		
porphyrin	subst	σ	σ^+	neutral	dication	shift[a]	neutral	dication	shift[a]
TNPP	$-NO_2$	0.81	0.79	424/424	447/453	23/29	646/645	655/657	9/12
TCMPP	$-CO_2CH_3$	0.47	0.48	418/419	444/447	26/28	645/644	655/656	10/12
TCPP	$-COOH$	0.44	0.42	NA/420	NA/447	NA/27	NA/645	NA/657	NA/12
TPP	$-H$	0.00	0.00	416/417	438/443	22/26	646/646	657/659	11/13
TTP	$-CH_3$	−0.14	−0.31	417/419	442/447	25/28	648/648	670/671	22/23
TMPP	$-OCH_3$	−0.28	−0.78	421/423	451/455	30/32	651/651	695/696	44/45
THPP	$-OH$	−0.22[b]	−0.92	419/424	452/458	33/34	648/653	706/711	58/58
TAPP	$-NH_2$	−0.57	−1.3	427/438	460/466	33/28	655/669	725/811	70/142
TDMAPP	$-N(CH_3)_2$	−0.63	−1.7	436/NA	470/477[c]	34/NA	663/NA	773/807[c]	110/NA

Fluorescence Data

		Hammett		fluorescence peak (nm)			Stokes shift (nm)	
porphyrin	subst	σ	σ^+	neutral	dication	shift[a]	neutral	dication
TNPP	$-NO_2$	0.81	0.79	NA/650	NA/699	NA/49	NA/5	NA/42
TCPP	$-COOH$	0.44	0.42	NA/650	NA/700	NA/50	NA/5	NA/43
TPP	$-H$	0.00	0.00	650/649	684/699	34/50	4/3	27/40
TTP	$-CH_3$	−0.14	−0.31	652/650	689/709	37/59	4/2	19/38
TMPP	$-OCH_3$	−0.28	−0.78	658/656	730/743	72/87	7/5	35/47
THPP	$-OH$	−0.22[b]	−0.92	654/661	740/760	86/99	6/8	34/49
TAPP	$-NH_2$	−0.57	−1.3	669/699	782/d	113/d	14/30	57/d
TDMAPP	$-N(CH_3)_2$	−0.63	−1.7	686/NA	d/d	d/d	23/NA	d/d

[a] Red shift between the corresponding bands of the neutral and dication porphyrin. [b] A "universal" value, among many suggested for the hydroxy group.[25] [c] In propylene carbonate rather than DMSO. [d] No fluorescence detected.

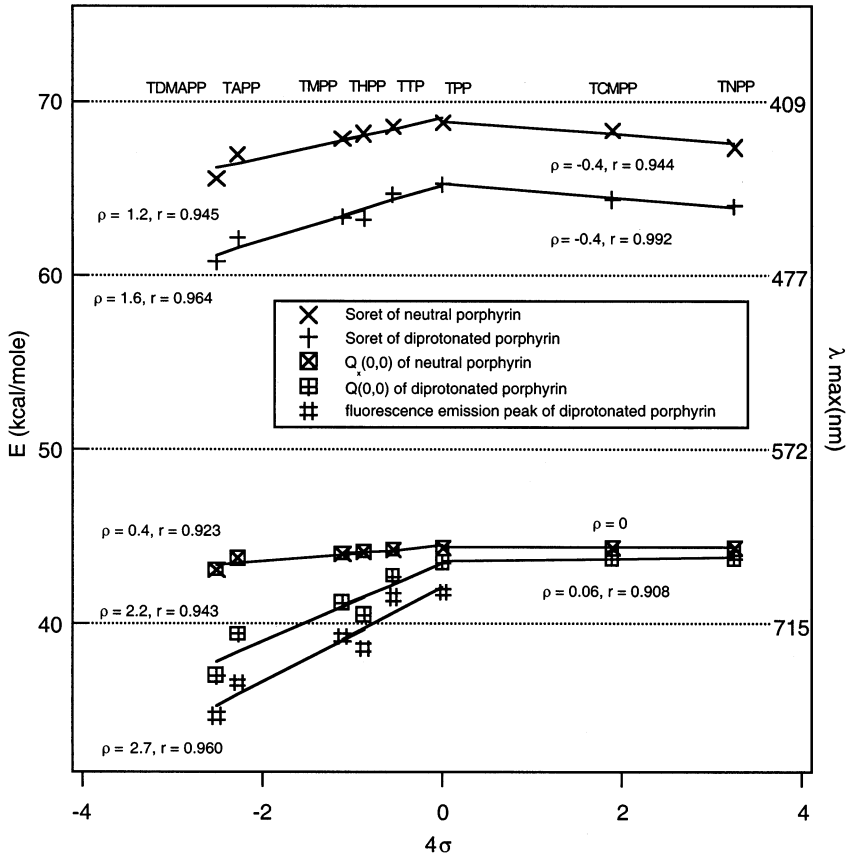

Figure 6. Absorption and emission data in DCM vs Hammett σ constants.

range and correlate with a trend to lower energy in more polar solvents. A tabulation of the data used for Figures 10 and 11 appears in the Supporting Information for this paper, along with a tabulation of the results of Hammett correlations in the different solvents.

An unexpected solvent effect was noted in DCM, in which light exposure in the presence of a porphyrin generated sufficient acid to significantly affect the spectrum. The effect was noted quantitatively by placing a dilute (4 μM) TTP solution in a diode array spectrophotometer; an effective acid titration could be observed simply by exposing the sample to the monitoring beam over a period of 2 min. The amounts of acid used for intentional titrations were not corrected for amounts photochemically generated; typical spectra were taken with a single pass, quickly

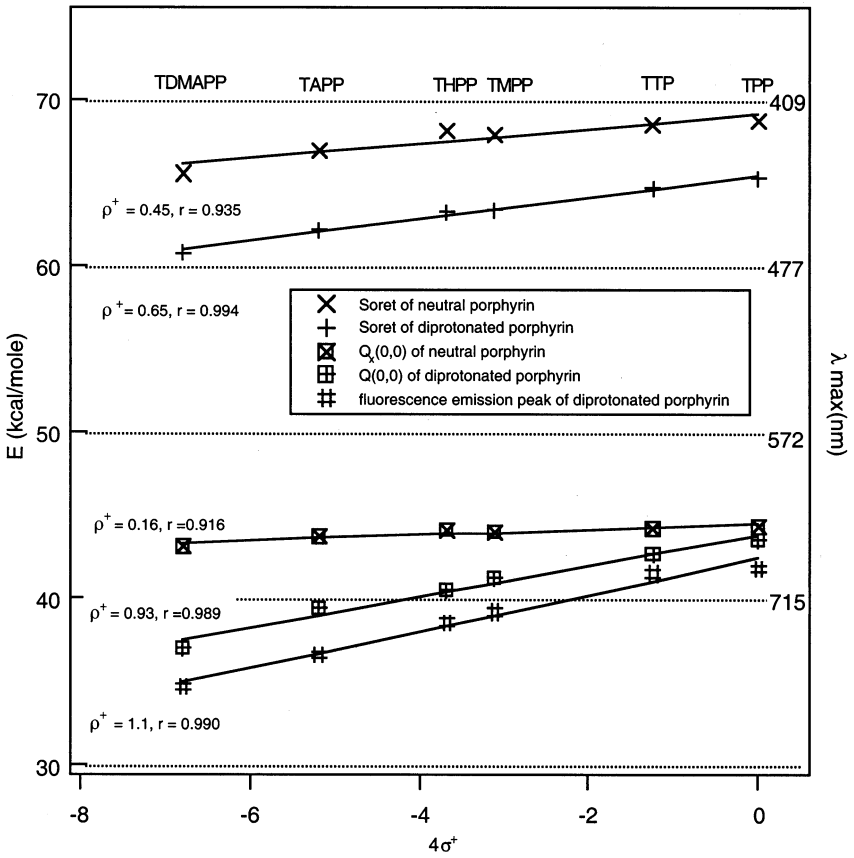

Figure 7. Absorption and emission data in DCM vs Hammett σ^+ constants.

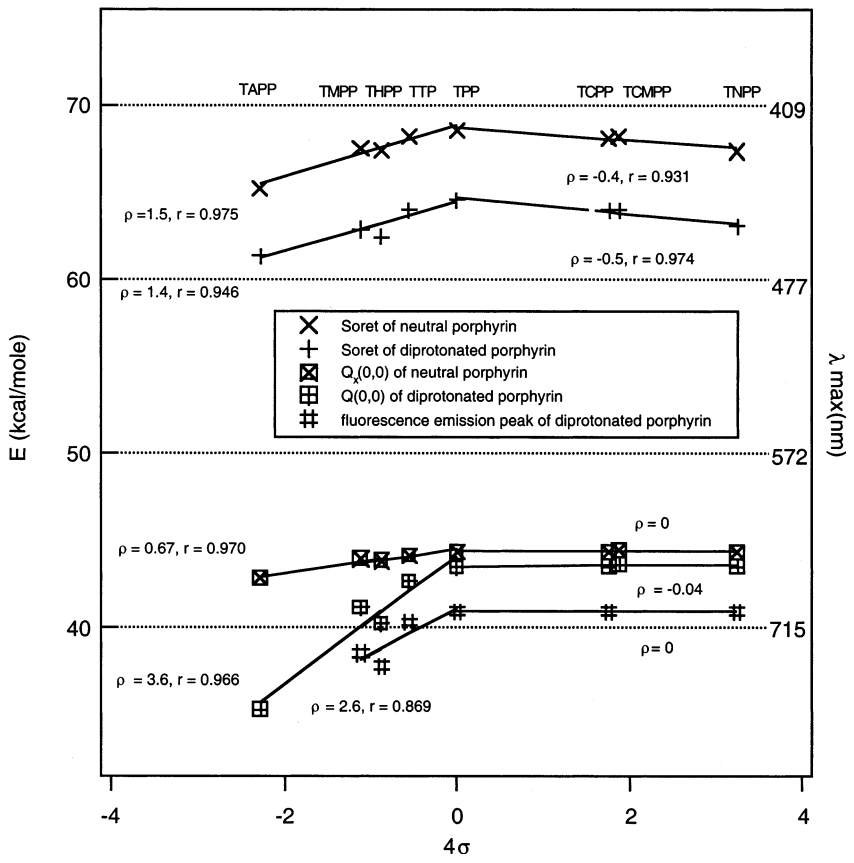

Figure 8. Absorption and emission data in DMSO vs Hammett σ constants.

enough that this should have been a minor effect. The release of HCl from chlorinated solvents is a well-known problem, but this photochemical generation may be a unique and potentially useful means of controlled release.

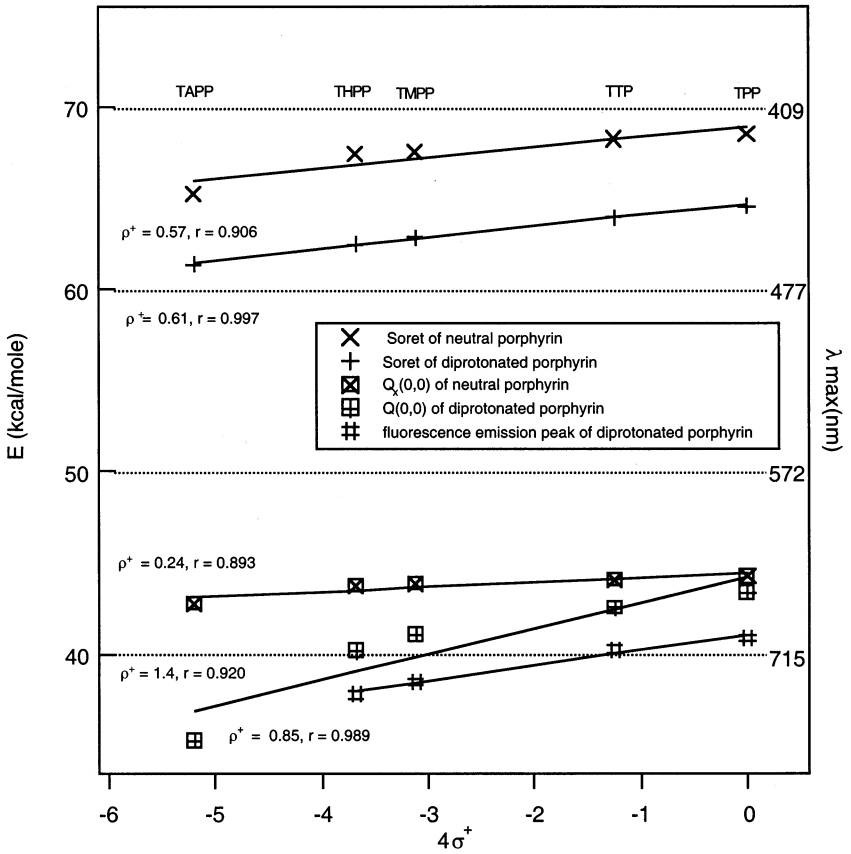

Figure 9. Absorption and emission data in DMSO vs Hammett σ^+ constants.

TABLE 2: Summary of Hammett Correlations (Boldfaced Values Represent the Better Linear Fit between ρ or ρ^+)

	DCM solvent		DMSO solvent	
	ρ e-donating/ e-withdrawing	ρ^+ e-donating only	ρ e-donating/ e-withdrawing	ρ^+ e-donating only
	absorption			
neutral, Soret	**1.2**/−0.4	0.45	**1.5**/−0.4	0.57
neutral, $Q_{x(0,0)}$	**0.4**/0	0.16	**0.7**/0	0.24
dication, Soret	1.6 /−0.4	0.65	1.4 /−0.5	**0.61**
dication, $Q_{(0,0)}$	2.2/0	0.93	3.6/0	**0.9**[a]
	emission			
dication, $Q_{(0,0)}$	2.7	**1.1**	2.6	**0.85**

[a] Excluding TAPP data; including those data, $\rho^+ = 1.4$, with a poorer correlation.

TABLE 3: Solvent Polarity Parameters

solvent	formula	E_T (30)	E_T^N	dielectric constant	bp (°C)
H_2O	HOH	63.1	1.000	78.5	100.0
MeOH	CH_3OH	55.4	0.762	32.6	64.7
ACN	CH_3CN	45.6	0.460	36.2	81.6
DMSO	$(CH_3)_2SO$	45.1	0.444	47.6	189.0
DMF	$HCON(CH_3)_2$	43.8	0.404	36.7	153.0
DCM	CH_2Cl_2	40.7	0.309	8.9	40.1
THF	cyclo-C_4H_8O	37.4	0.207	7.4	65.4

Effects of Mixed Substituents. Because all of the TPP derivatives initially studied for this work were symmetrically tetrasubstituted, it was considered desirable to investigate additional substitution patterns. Studies of TPPs with various numbers of dimethylamino substituents had been reported[19] and provided highly important information with respect to the roles of the substituents. TPPs with mixes of hydroxy and methoxy substituents were prepared, and their spectra were determined in DMSO solvent, as summarized in Table 4. Because the substituent effects of hydroxy and methoxy are very similar, the observed data were also very similar. However, it seems clear that the hydroxy substituent acts as the more electron-donating substituent in the context of the spectroscopic trends under consideration.

Discussion

Hyperporphyrin spectra that are based on substituent effects (rather than effects of central metal orbitals) are generally considered to arise from charge transfer transitions.[19] Recent molecular orbital calculations on TAPP and its protonated forms suggest that the effect originates from π orbitals that are primarily localized on the aminophenyl substituent.[21] These orbitals extend over the amino group as well as the phenyl π system and are calculated to correspond to the highest occupied molecular orbital (HOMO) and HOMO-1 for diprotonated TAPP (presumably additional calculations would locate all four of these orbitals—diprotonated monoamino TPP shows just a single aminophenyl orbital as its HOMO). The corresponding lowest unoccupied molecular orbital (LUMO) in these cases is a π^* orbital extending only over the porphyrin core. Thus, the lowest energy (hyperporphyrin) transition is assigned to π(phenyl) → π^*(porphyrin), which can be construed as a charge transfer transition. The reason the π(phenyl) orbital appears as the HOMO in these cases is a combination of the electron-donating effect of the amino group and the depression of core porphyrin π and π^* orbitals upon diprotonation. The π(phenyl) orbital is not calculated to be the HOMO or HOMO-1 in the cases of unsubstituted diprotonated TPP, neutral TAPP, fully protonated (+6) TAPP, or fully protonated (+3) monoamino TPP.[21]

Experimental data on the oxidation and reduction potentials for many of these same TPP derivatives have been reported.[9,10]

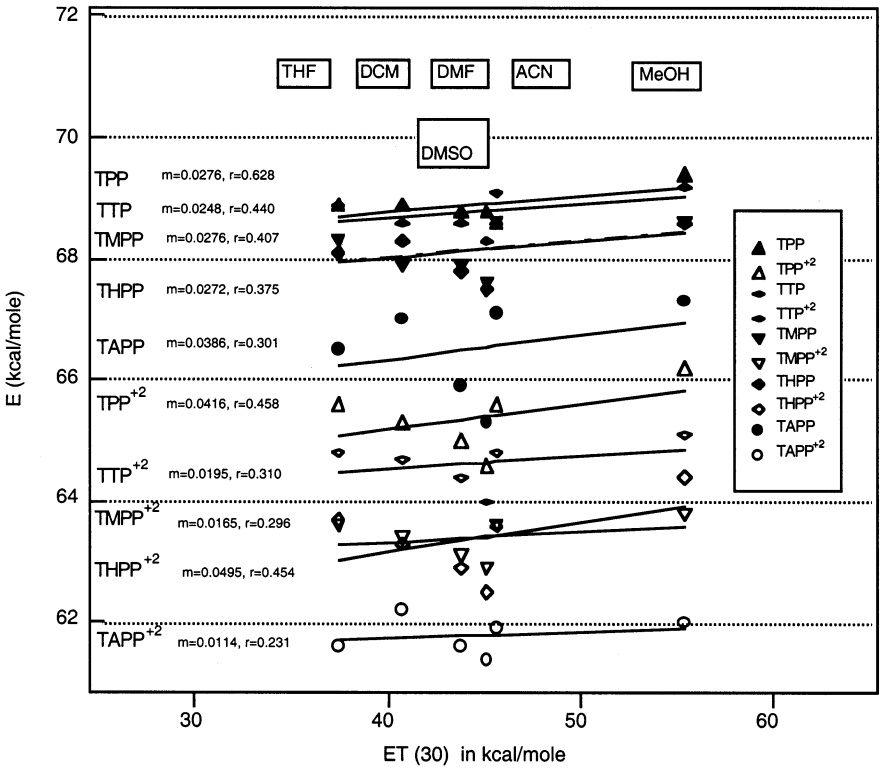

Figure 10. Solvent effects on the Soret band of neutral and diprotonated porphyrins.

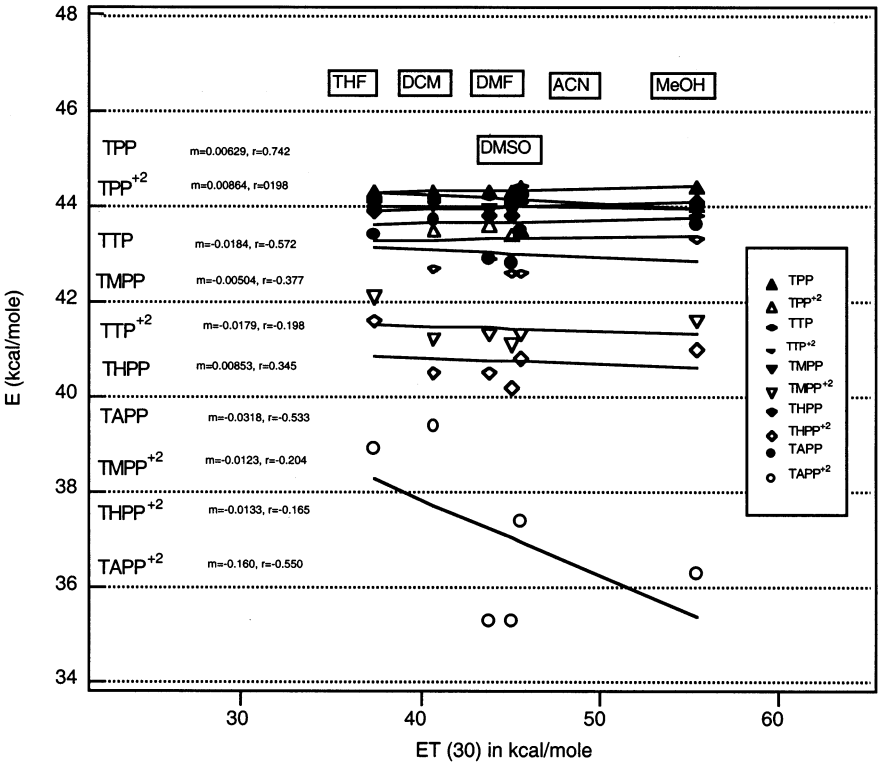

Figure 11. Solvent effects on the $Q(I)$ band of neutral and diprotonated porphyrins.

Increased electron donation leads the observed half-wave potentials (oxidation and two reductions) to shift to less positive potentials, all with slopes around 60 mV based on standard Hammett σ constants. These trends are interpreted as simple substituent effects on the energy levels of the porphyrin π orbital HOMO (one electron oxidation) and porphyrin π^* orbital LUMO (one electron reduction). The substituent effects must be mediated from the para position through the phenyl group to the porphyrin core, even though for the neutral TPPs these ring systems are distinctly noncoplanar. Because the observed substituents effects on the HOMO and LUMO run parallel, with comparable slopes, this implies a relatively constant transition energy, as is observed for most TPP derivatives. Indeed, Hammett plots for the $Q(I)$ transitions of substituted TPPs show very low slopes, as shown in Figures 6−9. However, oxidation potentials for the two most electron-donating substituents (THPP

TABLE 4: Absorption and Fluorescence Data for Mixed Substituent TPPs (All in DMSO Solvent)

Absorption Data

	Soret (nm)			$Q(I)$ (nm)		
porphyrin	neutral	dication	shift[a]	neutral	dication	shift[a]
TPP	417	443	26	646	659	13
TMPP	423	455	32	651	696	45
H_1M_3PP	423	455	32	649	700	51
H_2M_2PP	423	456	33	652	703	51
H_3M_1PP	424	457	33	651	707	56
THPP	424	458	34	653	711	58

Fluorescence Data

	fluorescence peak (nm)			Stokes shift (nm)		isosbestic	fluorescence	
porphyrin	neutral	dication	shift[a]	neutral	dication	excit (nm)	rel yield	lifetime (ns)
TPP	649	699	50	3	40	427	0.30	9.3
TMPP	656	743	87	5	47	434	0.18	8.6
H_1M_3PP	657	750	93	8	50	434	0.15	8.5
H_2M_2PP	658	749	91	6	46	434	0.13	8.5
H_3M_1PP	658	755	97	7	42	435	0.11	8.4
THPP	661	760	99	8	49	436	0.12	8.4

[a] Red shift between the corresponding bands of the neutral and dication porphyrin.

TABLE 5: Oxidation−Reduction Data and Prediction of Transition Energies

porphyrin	subst	Hammett σ	E(ox)[a] (V)	E(red)[a] (V)	calcd[b] ΔE (eV)	neutral $Q(I)$ (eV)	dication $Q(I)$ (eV)
TCMPP	$-CO_2CH_3$	0.47	1.14	−0.92	2.06	1.93	1.89
TPP	−H	0.00	1.04	−1.03	2.07	1.92	1.88
TMPP	$-OCH_3$	−0.28	0.94	−1.08	2.02	1.90	1.78
THPP	−OH	−0.38	0.75	−1.12	1.87	1.90	1.74
TAPP	$-NH_2$	−0.57	0.48	−1.18	1.66	1.85	1.53

[a] Oxidation and reduction data are half-wave potentials measured in DMSO by cyclic voltammetry.[10] [b] Calculated transition energies are simply the difference between E(ox) and E(red).

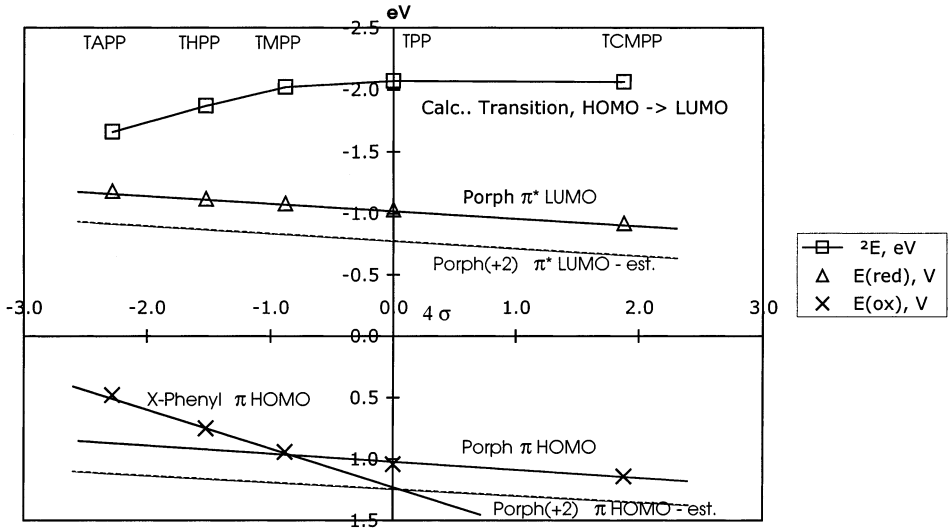

Figure 12. HOMO and LUMO energy levels estimated from measured oxidation and reduction potentials of the neutral porphyrins.[10] Corresponding levels for diprotonated porphyrins are estimated (dashed lines) to illustrate the lower energy transitions observed in the dications.

and TAPP) are substantially lower (less positive) than predicted, i.e., there is a HOMO higher in energy than predicted based simply on substituent effects on the porphyrin. The interpretation is that substituent effects in these cases are acting directly on the phenyl ring to which they are attached, and they affect the oxidation potential strongly because this orbital has become the HOMO.

Table 5 shows measured oxidation and reduction potentials for selected substituted TPPs in DMSO and calculates a transition energy based simply on the difference between them. Figure 12 illustrates these trends, assigning the oxidation potential to the HOMO energy level and the reduction potential to the LUMO energy level. In this illustration, the hyperporphyrin effect can be seen as a crossing of the phenyl π orbital over the porphyrin π orbital, creating a different HOMO and thereby a charge transfer transition at lower energy. The crossing apparently occurs at about the position of TMPP, corresponding to the break in the Hammett plot observed for oxidation potentials.[10] An estimate of the energy level changes brought about by diprotonation is illustrated with the dashed lines. On the basis of the shifts observed in the hyperporphyrin cases, a shift of about +0.2 eV from neutral to dication is applied to the porphyrin orbitals but not the phenyl orbitals. If this is the case, the crossing of the phenyl π orbital over the porphyrin π orbital occurs at about the position of TPP, as is observed with the Hammett plots of dication $Q(I)$ bands (Figures 6−9).

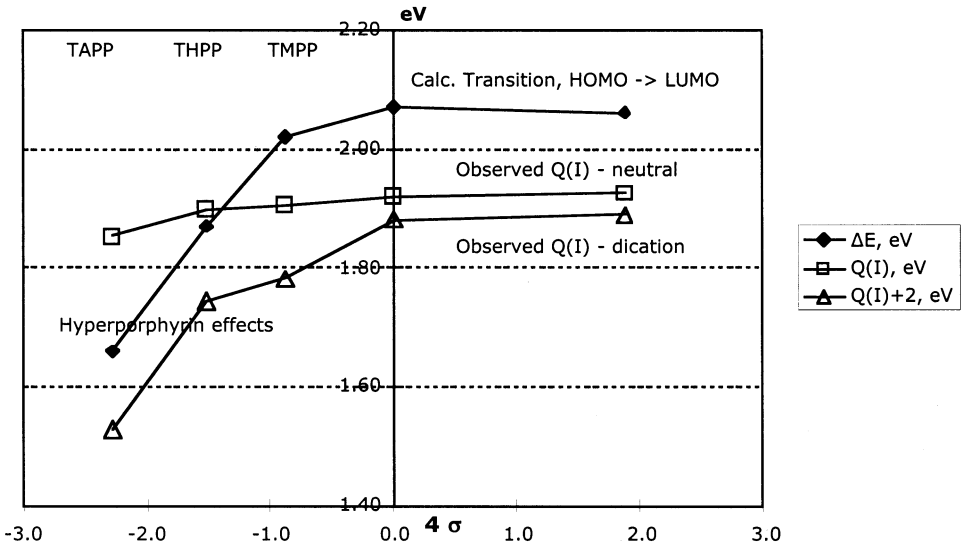

Figure 13. Comparison of observed $Q(I)$ transition energies (in eV) with those calculated from oxidation and reduction potentials for neutral porphyrins (as in Figure 12). The lines simply connect the points.

Figure 13 compares the calculated transition energies with the observed $Q(I)$ bands for both the neutral and the diprotonated porphyrins. In the case of the dications, the calculated values follow the observed trend very well, although the calculated values are uniformly high by about 0.2 eV. In the case of neutral TPPs, the calculation predicts a hyperporphyrin effect much stronger than is observed (or earlier than is observed).

Acknowledgment. The majority of this work comprised the M.S. Thesis project of J.R.W. Additional experimental work was done by S.W.C., sponsored by the Research Corporation Partners in Science Program, by A.S. and Mary Ann Brennan, who were sponsored by the Apprenticeships in Science and Engineering Program, and by Nick Shults and HongDiem Thi Nguyen. ICR-MS spectra were taken at the Pacific Northwest National Laboratories Environmental Molecular Sciences Lab Facilities through the cooperation of Dr. Gordon Anderson. MALDI-MS spectra were taken at Washington State University LBB2 Analytical Services Laboratory through the cooperation of Dr. William Siems. Fluorescence lifetime measurements were performed at the University of Texas Fast Kinetics Laboratory through the cooperation of Professor Stephen Webber or at Spex Industries through the cooperation of Dr. Sal Atzemi. Synthetic assistance was provided by Dr. Peter Pessiki of The Evergreen State College. Helpful correspondence and sharing of unpublished data with Professor Henry Linschitz and Dr. Hong Wang of Brandeis University and discussions with Professor Martin Gouterman of The University of Washington are gratefully acknowledged. Partial funding of the work came from the U.S. Department of Energy Basic Energy Sciences/Solar Photochemistry Program, Grant No. DE-FG06-90ER14131, and from the Portland State University Faculty Development Program.

Supporting Information Available: Tables of peak wavelengths and Hammett values. This material is available free of charge via the Internet at http://pubs.acs.org.

References and Notes

(1) *The Porphyrin Handbook*; Kadish, K. M., Smith, K. M., Guilard, R., Eds.; Academic Press: San Diego, 2000.

(2) Gouterman, M. Optical Spectra and Electronic Structure of Porphyrins and Related Rings. In *The Porphyrins*; Dolphin, D., Ed.; Academic Press: New York, 1978; Vol. III, pp 1−165.

(3) Akins, D. L.; Zhu, H.; Guo, C. *J. Phys. Chem.* **1996**, *100*, 5420−5425.

(4) Hambright, P. Chemistry of Water-Soluble Porphyrins. In *The Porphyrin Handbook*; Kadish, K. M., Smith, K. M., Guilard, R., Eds.; Academic Press: New York, 2000; Vol. 3, pp 129−210.

(5) Clarke, S. E.; Wamser, C. C.; Bell, H. E. *J. Phys. Chem. A* **2002**, *106*, 3235−3242.

(6) http://www-chem.ucdavis.edu/groups/smith/chime/Porph_Struct/start_here.html, accessed August 2002.

(7) Silvers, S. J.; Tulinsky, A. *J. Am. Chem. Soc.* **1967**, *89*, 3331−3337.

(8) Stone, A.; Fleischer, E. B. *J. Am. Chem. Soc.* **1968**, *90*, 2735−2748.

(9) Kadish, K. M.; Morrison, M. M. *J. Am. Chem. Soc.* **1976**, *98*, 3326−3328.

(10) Ransdell, R. A.; Wamser, C. C. *J. Phys. Chem.* **1992**, *96*, 10572−10575.

(11) Meot-Ner, M.; Adler, A. D. *J. Am. Chem. Soc.* **1972**, *94*, 4763−4764.

(12) Meot-Ner, M.; Adler, A. D. *J. Am. Chem. Soc.* **1975**, *97*, 5107−5110.

(13) Dalton, J.; Milgrom, L. R.; Pemberton, S. M. *J. Chem. Soc., Perkins II* **1980**, 370−372.

(14) Traylor, T. G.; Nolan, K. B.; Hildreth, R. *J. Am. Chem. Soc.* **1983**, *105*, 6149−6151.

(15) Li, M.; Chen, X.-Y.; Zou, J.-Z.; Xu, Z.; You, X.-Z. *Chin. J. Chem.* **1996**, *14*, 20−24.

(16) Milgrom, L. R.; Yahioglu, G.; Jogiya, N. N. *Free Radical Res.* **1996**, *24*, 19−29.

(17) Datta-Gupta, N.; Bardos, T. J. *J. Heterocycl. Chem.* **1966**, *3*, 495−502.

(18) Gunter, M. J.; Robinson, B. C. *Aust. J. Chem.* **1989**, *42*, 1897−1905.

(19) Ojadi, E. C. A.; Linschitz, H.; Gouterman, M.; Walter, R. I.; Lindsey, J. S.; Wagner, R. W.; Droupadi, P. R.; Wang, W. *J. Phys. Chem.* **1993**, *97*, 13192−13197.

(20) Udal'tsov, A. V.; Kazarin, L. A. *J. Photochem. Photobiol. A* **1996**, 99−107.

(21) Vitasovic, M.; Gouterman, M.; Linschitz, H. *J. Porphyrins Phthalocyanines* **2001**, *5*, 191−197.

(22) Momenteau, M.; Mispelter, J.; Loock, B.; Bisagne, E. *J. Chem. Soc., Perkin Trans. 1* **1983**, *1*, 189−196.

(23) Adler, A. D.; Longo, F. R.; Finarelli, J. D.; Goldmacher, J.; Assour, J.; Korsakoff, L. *J. Org. Chem.* **1967**, *32*, 476−478.

(24) Reichardt, C. *Solvents and Solvent Effects in Organic Chemistry*; VCH: Weinheim, Germany, 1988.

(25) Exner, O. A Critical Compilation of Substituent Constants. In *Correlation Analysis in Chemistry*; Chapman, N. B., Shorter, J., Eds.; Plenum Press: New York, 1978; pp 439−489.